ACS APPLIED MATERIALS & INTERFACES

Research Article

www.acsami.org

Permission to Enter Cell by Shape: Nanodisk vs Nanosphere

Yi Zhang,[†] Samuel Tekobo,[‡] Ying Tu,[§] Qunfang Zhou,[§] Xinlong Jin,[§] Sergey A. Dergunov,[‡] Eugene Pinkhassik,[‡,#] and Bing Yan*[,†]

[†]School of Chemistry and Chemical Engineering, Shandong University, Jinan 250100, China

[‡]Department of Chemistry and Institute for Nanomaterials Development and Innovation at the University of Memphis (INDIUM), University of Memphis, Memphis, Tennessee 38152, United States

[§]Department of Chemical Biology and Therapeutics, St. Jude Children's Research Hospital, Memphis, Tennessee 38105, United States

[#]Department of Chemistry, Saint Louis University, St. Louis, Missouri 63103, United States

Supporting Information

ABSTRACT: Changing polystyrene nanoparticles from three-dimensional spherical shape to two-dimensional disk shape promotes their cell surface binding with significant reduction of cell uptake. As a result of lower cell uptake, nanodisks show very little perturbations on cell functions such as cellular ROS generation, apoptosis and cell cycle progression compared to nanospheres. Therefore, disk-shaped nanoparticles may be a promising template for developing cell membrane-specific and safer imaging agents for a range of biomedical applications such as molecular imaging, tissue engineering, cell tracking, and stem cell separation.

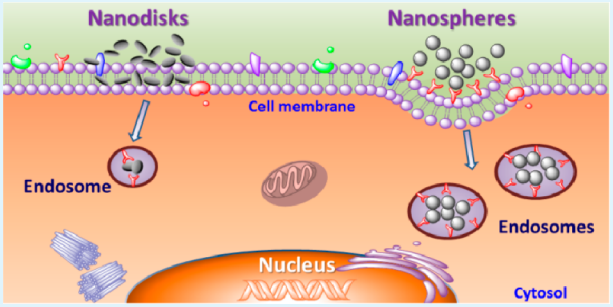

KEYWORDS: *nanodisk, membrane permeability, cell uptake, cytotoxicity*

INTRODUCTION

Human control of nanoparticle's biological activity is imperative since nanomaterials are increasingly used in various industries, medicine, environment, and consumer products. It is recognized that nanoparticles' toxicity and their many useful biological properties are related to their fundamental properties such as their size, shape, core material, and surface properties. These have been explored, but many unknowns still remain to be discovered. Nanoparticles can be internalized by cells via different pathways.[1−3] Inside cell, these nanoparticles may cause cytotoxicity. Although cell internalization of nanoparticles is necessary for applications like drug or gene delivery, this is not desirable when it induces cytotoxicity.

Cell labeling and tracking are currently practiced using organic dyes[4] or spherical nanoparticles with magnetic or fluorescent properties.[5−7] Compared to organic dyes, nanoparticles show advantages in terms of imaging sensitivity,[8] photochemical stability,[9] and multifunctionalization.[10] The molecular imaging agents ideally bind to cell surface, yet are not internalized. However, current imaging agents, organic dyes or spheric nanoparticle,[11−15] all enter cells significantly and induce cytotoxity to various degrees.

Cell internalization can be prevented by nanoparticle's surface chemistry such as PEGylation[16] and dextran modifications.[17] PEGylated nanoparticles have a weaker interaction/association with the cell membranes and a reduced internalization.[2] Although this decreases their potential toxicity, it also deprives their functions like imaging and cell tracking because both of these functions require membrane bindings. It has been demonstrated that the shape of nanoparticles played an important role in their internalization in macrophage.[18] We speculate that conversion of three-dimensional nanoparticle to a two-dimensional shape may offer larger contact surface with cell membranes while generate less impact during their interactions. These disk-shaped nanoparticles may bind to, but are not internalized by cells. To test this hypothesis, we investigated polystyrene nanospheres and nanodisks with the same diameter and identical surface chemistry for their interactions with human cells. We found that nanospheres enter cells and perturb cellular functions, whereas nanodisks bind only to cell membrane with a significantly reduced cellular perturbation.

EXPERIMENTAL SECTION

Cell Cultures, Materials, And Reagents. All cell lines were purchased from ATCC (Manassas, VA). HeLa, Hek 293 and BJ cells were grown in Dulbecco's Minimum Essential Medium (DMEM, from Gibco, Grand Island, NY) supplemented with 10% fetal bovine serum (Invitrogen, Carlsbad, CA), 2 mM L-glutamine, 100 μg/mL penicillin, and 100 U/mL streptomycin. Jurkat cells (Clone E6−1) were grown in Roswell Park Memorial Institute (RPMI) Medium 1640, with the

Received: May 17, 2012
Accepted: July 26, 2012
Published: July 27, 2012

same supplements as those for DMEM. All cells were grown in a humidified incubator at 37 °C (95% humidity, 5% CO_2). Carboxyl nanospheres, 20 nm (C37261) and FluoSpheres carboxylated nanospheres, 20 nm, yellow-green fluorescent (505/515) (F8787) were purchased from Invitrogen. Laurdan (6-dodecanoyl-2-dimethylaminonaphthalene) was purchased from AnaSpec, Inc.

Synthesis of Nanodisks. The synthetic process of nanodisks was previously introduced.[19] Briefly, a bicelle solution (15%, composed of 1,2-Dimyristoyl-sn-Glycero-3-Phosphocholine (DMPC) and 1,2-dihexanoyl-sn-glyc- ero-3-phosphocholine (DHPC) with a ratio of 3:1) was prepared by mixing 500 μL of DMPC solution (123 mg, 0.181 mmol) and 500 μL of DHPC solution (27 mg, 0.06 mmol) in 10 mM phosphate buffer (pH 6.5). The mixture was gently shaken and centrifuged at 4000 *g* until a clear solution was obtained. Styrene (6 μL, 0.055 mmol) and divinylbenzene (8 μL, 0.055 mmol) were added to the bicelle solution, and the mixture was gently stirred for 48 h at 36 °C. The styrene−divinylbenzene molar ratio was 1:1 and the total monomer− lipid ratio was 0.46:1. The solution was placed in a quartz cuvette and 0.6 mg of a photochemical initiator Lucirin TPO was added (1.4% molar equivalent of monomers). The sample was irradiated in a Rayonet photocabinet equipped with eight 254 nm lamps. To monitor polymerization, 5 μL aliquots were taken every 10 min, diluted with 4 mL chloroform, and UV absorbance was measured at 282 and 291 nm by the Agilent 8453 UV−vis spectrophotometer (Agilent Technologies, Santa Clara, CA) to determine the amount of residual monomer. These results were corroborated by gas chromatography (GC) analysis of monomers extracted into hexane. After 90 min of irradiation, the sample was mixed with 10 mL methanol and centrifuged at 4000 *g* for 1 min. Methanol was carefully decanted, and this methanol washing step was repeated 5 times. After the final washing step, the precipitate was dried to yield 9 mg (76%) of white powder.

For tracking cell membrane association or internalization, fluorescein-labeled nanodisks are synthesized following the reported methods[20,21] with slight modifications. Briefly, *t*-butylstyrene (20 μL, 1.09×10^{-4} mol), *p*-divinylbenzene (16 μL, 1.12×10^{-4} mol), fluorescein-O-methacrylate (19.1 mg, 4.77×10^{-5} mol), and photoinitiator 2,2-dimethoxy-2-phenylacetophenone (3 mg, 0.117×10^{-5} mol) were added to chloroform solution of 1,2-dimyristoyl-sn-glycero-3-phosphocholine (DMPC) (18×10^{-5} mol, 122 mg) and 1,2-dihexanoyl-sn-glycero-3-phosphocholine (DHPC) (6×10^{-5} mol, 27.1 mg). Chloroform was evaporated using a stream of purified argon to form a lipid/monomer film on the wall of a culture tube. The lipid film was further dried under vacuum for 30 min to remove traces of chloroform. The dried film was hydrated with 1 mL of a 0.01 M Tris buffer solution (pH 7.4) giving a dispersion of multilamellar vesicles. Five repeated freeze−thaw cycles were carried out by plunging the flask into isopropanol (cooled with dry ice) followed by slow heating above the phase transition temperature (about 40−45 °C). Sample was sonicated for 1 min after every freeze−thaw cycle. Transparent and viscous solution was obtained. The suspension was irradiated during 100 min with UV light (254 nm) in a photochemical reactor (10 lamps, 32W each; the distance between the lamps and the NCs was 10 cm) using quartz tube with path length of light of approximately 3 mm. Polymer was precipitated with methanol, washed 4 times in methanol with centrifugation and was freeze-dried to powder. For cell experiment, polymer nanoparticles were suspended in 10% fetal bovine serum in water to a final concentration of 1.0 mg/mL. The suspensions were sonicated in an ultrasonic cleaner (FS-60) for 15 min to further disperse nanoparticles and it is sonicated again immediately before use.

Transmission Electron Microscopy Imaging, Dynamic Light Scattering, and Zeta Potential Measurement. Transmission electron microscopy (TEM) imaging was performed with the JEOL JEM-1200EXII transmission electron microscope (JEOL USA, Peabody, MA) at a working voltage of 100 kV. To prepare the sample, A drop of sample was carefully placed on a 200-mesh carbon grid and excess sample was wiped away with filter paper. Then a drop of 2% phosphotungstic acid (pH 6.2) was added to the grid to negatively stain the sample. After 2 min, the excess liquid was wiped off. Dynamic light scattering (DLS) measurement using a disk[22] or sphere model was made by the Dynapro Titan DLS (Wyatt Technology Corporation, Santa Barbara, CA, USA) after a filtration step with a 0.22 μm filter. The Zeta potential of nanoparticles was determined using Zetasizer Nano-Z (Malvern Instruments, Worcestershire, UK). The analysis was performed at 25.0 ± 0.2 °C using sample solutions in deionized distilled water or in 10% fetal bovine serum. The DLS and Zeta potential results were average values of three independent measurements.

Confocal Fluorescence Laser Microscopy and Flow Cytometry. To study the cell membrane association or internalization using confocal laser scanning microscopy (CLSM), 50 000 HeLa cells were seeded in a 35 mm Petri dish with 10 mm glass-bottom microwell. After overnight incubation at 37 °C, nanoparticle suspension was added to cells with a final concentration of 50 μg/mL. At 10 min and 2 h, the medium was decanted and cells were washed thrice with phosphate-buffered saline (PBS, pH 7.4) to fully remove free nanoparticles. Cells were then fixed with freshly prepared 4% paraformaldehyde for 30 min at 4 °C. Paraformaldehyde was washed out with PBS and 10 μg/mL of Alexa Fluor 647 conjugated wheat germ agglutinin (WGA-647) was added to the microwell to stain the cell membrane for 5 min at room temperature in darkness. Cells were then washed thrice again with PBS followed by counter staining with DAPI in mounting medium. Samples were immediately examined under the Leica (Nussloch, Germany) TCS confocal laser scanning microscope.

To measure the cell uptake, 200 000 HeLa/well were seeded to a 12-well plate and after overnight incubation at 37 °C, nanoparticles was added to final concentration of 50 μg/mL. Cells were washed with PBS thrice to remove free nanoparticles followed by digestion with 0.05% trypsin at specified times. The harvested cells were analyzed under the Expresspro model with the Guava EasyCyte Mini flow cytometry system (Millipore, Billerica, MA). Green fluorescence was monitored.

Permeation Experiments. PAMPA assay was carried out following manufacture's protocol at pH 7.4 (PAMPA Explorer, Double-Sink and Gut-Box, pION). To avoid the interference of nanoparticles on ultraviolent assay, fluorescence measurement was used to quantify nanoparticles in each section. The value of retained/permeable was the ratio of the amount of nanoparticles retained by the membrane vs that permeabilized.

The effective permeability coefficients P_e (cm/s) were calculated using the published equation as below[23]

$$P_e = \frac{2.303 V_D}{A(t - \tau LAG)}\left(\frac{V_A}{V_A + V_D}\right) \times \log\left[1 - \left(\frac{V_A + V_D}{V_D(1 - R)}\right)\frac{C_A(t)}{C_D(0)}\right]$$

where t is incubation time (30 min in this experiment), V_A and V_D are the volumes of the acceptor and the donor wells, R is the membrane retention factor, $C_A(t)$ and $C_D(t)$ are the concentrations of the nanoparticles (mg/mL) in the acceptor and donor wells at time t as measured by fluorescence intensity, $C_D(0)$ is the concentration of the nanoparticles (mg/mL) in the donor well at time 0, and A is the filter area multiplied by a nominal porosity of 70% according to the manufacturer. τ_{LAG} is the steady-state time (s), that is, the time needed for the permeant's concentration gradient to become stabilized, which are short relative to the total permeation time (30 min with unstirred plates) and for this reason they were considered negligible in this study.

Detection of the Ordering of Phospholipids in Cell Membrane. HeLa cells were seeded in 96-well plates at the density of 20 000 cells/well. After 24 h, the cells were prelabeled with the Laurdan dye (0.4 μM) for 1 h in the incubator. Then, the dye solution was removed and the cells were rinsed with PBS (37 °C). The wells were then refilled with medium containing nanoparticles. Before assay, the incubator of Spectramax M5 multiplate reader (Molecular Device) was set to "on" and the temperature was set to 37 °C. After the addition of nanoparticles, 96-well plate was immediately mounted to the chamber of Spectramax M5 multiplate reader. After incubation for 10, 50, 120, 180, 260 min, the fluorescence intensity was scanned from

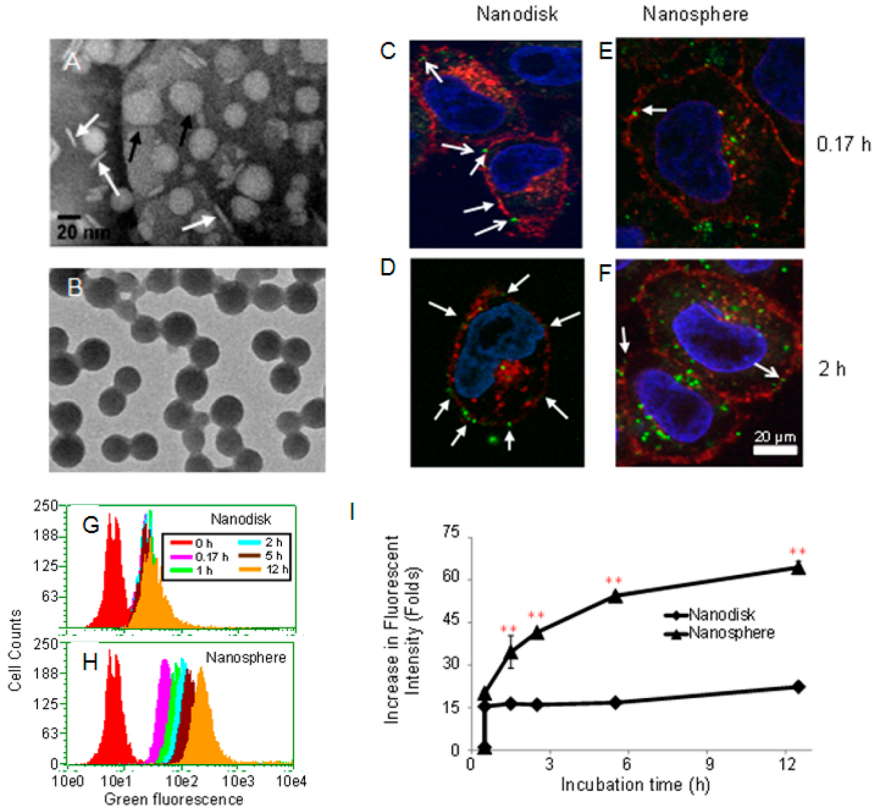

Figure 1. (A, B) TEM images of (A) nanodisks and (B) nanospheres. In A, black arrow indicated nanodisks lying flat and white arrow indicated those standing on the edge. (C–I) Cell uptake of two polymeric nanoparticles. (C–F) Subcellular localization of both nanoparticles in HeLa cells. HeLa cells were exposed to 50 μg/mL of both nanoparticles for 0.17 and 2 h and cells were fixed for confocal laser scanning microscopic observation. At both time points, nanospheres were mostly found internalized in cells while nanodisks bind on the cell membrane. The white arrows indicated the nanoparticles on cell membrane (red, cell membrane; green, nanoparticles; blue, cell nucleus). (G, H) HeLa cells were exposed to 50 μg/mL of both nanoparticles for different times and cell membrane association or internalization was analyzed by flow cytometry. (I) Quantification of the cell membrane association or internalization of both nanoparticles after normalization with the relative fluorescence intensity ($F_{Nanodisk}$:$F_{Nanosphere}$ = 1:4.9) (** < 0.001).

Table 1. Characterizations of Nanoparticles

			Zeta potential (mV)		avg hydrodynamic diameter (by DLS, nm)	
	chemical composition	diameter (nm)	in H_2O	in 10% fetal bovine serum	in H_2O	in 10% fetal bovine serum
nanodisk	polystyrene	19.7 ± 4.6	−13.6 ± 1.78	−23.4 ± 1.32	225 ± 20	40 ± 8
nanosphere	polystyrene	20.6 ± 2.4	−16.8 ± 0.46	−24.3 ± 0.67	150 ± 14	80 ± 6

400 to 500 nm using excitation wavelength of 340 nm.[24] In all time points, no wavelength shift was found and the peak wavelength was at 451 nm. So the fluorescence intensity of Laurdan dye at 451 nm represents the most ordered phospholipid of cell membrane.[24] Because the maximal intensity of Laurdan dye in chaotic phospholipids was typically at 490 nm,[25] the fluorescence intensity at 490 nm represents the least ordered phospholipids in this study. The ordering of phospholipids in cell membrane was scaled by generalized polarization (GP) value, which was calculated as GP = $(I_{451} - I_{490})/(I_{451} + I_{490})$, where I_{451} and I_{490} are respectively the fluorescence intensity of Laurdan dye at wavelengths of 451 and 490 nm.

Reactive Oxygen Species (ROS) Assay. Cells were seeded in 12-well plates at the density of 200 000 cells/well for Hek 293 and Jurkat cells and 100 000 cells/well for BJ cells. After overnight incubation, stock suspensions of nanoparticles were added to cells to final concentrations of 50 and 400 μg/mL for another 24 h incubation. Cells were then incubated with culture mediumthat contained 5 μM dihydroethidium (DHE) for 30 min at 37 °C. All cells were then washed with PBS twice and Hek 293 and BJ were digested with 0.05% trypsin. ROS generation was analyzed by flow cytometry on a Guava EasyCyte Mini Flow Cytometry system. Red fluorescence was monitored.

Cell Apoptosis Assay. Cells were seeded in 12-well plates at a density of 3 × 10^5 cells/well in 1.0 mL DMEM medium with the exception for Jurkat cells, which were incubated with RPMI 1640 medium. After 24 h incubation, nanoparticles were added to final concentrations of 50 and 400 μg/mL. HeLa, Hek 293 and BJ cells were trypsinized 24 h later. Floating cells were collected and suspended in 2.0 mL PBS. Cells were further stained with Guava Nexin-V reagent per manufacturer's instructions, followed by flow cytometry analysis.

Cell Cycle Analysis. Cells were seeded into 6-well plates at a density of 500,000 cells/well. After 24 h incubation, nanoparticle suspensions were added to final concentrations of 50 and 400 μg/mL. After 24 h, HeLa, Hek 293 and BJ cells were trypsinized. All cells were aspirated, and counted. Cells were centrifuged, washed with PBS, and stained with Guava cell cycle reagent for 30 min at room temperature in darkness prior to flow cytometry analysis.

RESULTS AND DISCUSSION

Monodispersed Nanodisks and Spherical Nanoparticles. Polymeric nanodisks were synthesized as previously reported.[19,26] They have a diameter of 20 nm, the same as the

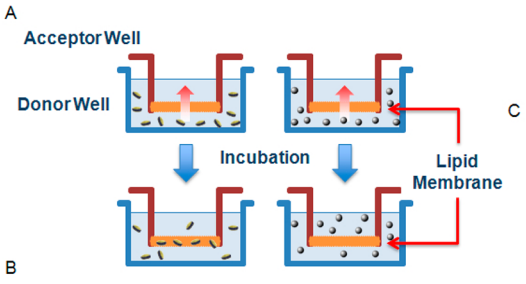

Nanoparticles (ug/mL)	Permeability (10^{-6} cm/s)	Membrane/Permeable
Nanodisk (400)	4.1 ± 2.5 *	0.19 ± 0.05 *
Nanodisk (50)	4.0 ± 2.1 *	0.15 ± 0.045 *
Nanosphere (400)	24.9 ± 6.2	0.023 ± 0.0009
Nanosphere (50)	27.6 ± 7.5	0.017 ± 0.0014

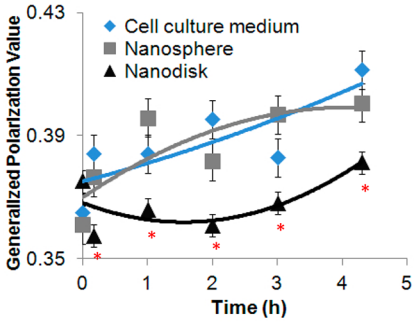

Figure 2. Nanodisks bind on cell surface and reduce lipid ordering of cell membrane. (A) Schematic diagram showing the working model of parallel artificial membrane permeability assay (PAMPA) method. (B) Different permeabilities of two nanoparticles assayed by PAMPA method. Artificial membrane permeabilities were assayed under two concentrations (50 and 400 μg/mL). Higher percentage of nanodisk is retained by artificial membrane shown by higher retained/permeable nanoparticles value and nanodisks exhibit a lower permeability in comparison with nanospheres (* $p < 0.05$, compared to nanospheres). (C) Nanodisks but not nanospheres reduce lipid ordering of cell membrane in HeLa cells. The phospholipid ordering of cell membrane was scaled by the generalized polarization (GP) value, which was calculated as introduced in the materials and methods. A lower GP value represents more fluid state of phospholipid bilayer. The increase in the GP values with time in all groups indicated the natural aging of cell membrane[25](* $p < 0.05$, nanodisks compared to untreated group).

diameter of polystyrene nanospheres used in this work (see Figure S1 in the Supporting Information). TEM images and small-angle neutron scattering measurements[27] show that nanodisks have a disk shape with a diameter of about 20 nm and thickness of 2 nm (Figure 1A). Nanospheres show uniform spherical shape by TEM (Figure 1B). The electrostatic property of nanoparticles was characterized by Zeta potentials. The Zeta potentials of nanodisks and nanospheres were −13.6 and −16.8 mV in water and −23.4 and −24.3 mV in serum, suggesting that the protein adsorption increases their surface negative charges in a similar fashion (Table 1). In order to get monodispersed nanoparticle solutions, they were dispersed in 10% fetal bovine serum. After sonication, DLS analysis showed that nanodisks had a hydrodynamic diameter of 40 nm, in comparison with 80 nm for nanospheres. Considering the protein corona on the nanoparticles' surface,[28] these nanoparticles were not heavily aggregated and some of them were even monodispersed under our experimental conditions.

Unlike Nanospheres, Nanodisks Seldom Enter Cells. Using HeLa cell as a human cell model, we first evaluated nanoparticle-cell interactions and cell membrane association/internalization. Both nanodisks and nanospheres were covalently labled with a tiny fraction of fluorescein. After fluorescein labeling, the surface charges and diameters of both nanoparticles remain the same (see Table S1 in the Supporting Information). Nanospheres have more binding sites and exhibit a 4.9-fold higher fluorescence intensity compared to nanodisks at the same particle concentration (Figure S2). Examination by CLSM revealed that nanospheres were internalized by HeLa cells, whereas nanodisks were mainly associated with cell membranes (Figure 1C−F and Figure S3 in the Supporting Information). Flow cytometry analysis showed that nanodisk-cell membrane association quickly reached a plateau at 10 min and there was not much change in the next 12 h. Nanosphere-cell internalization slowly reached saturation in about 10 h (Figure 1 G,H). At 12 h, the fluorescence intensity of nanosphere-incubated cells was 2.9 fold higher than that of nanodisks (Figure 1I). This was probably due to the fact that nanodisks mainly associated with cell membranes while nanospheres entered cells in addition to cell membrane binding.

To substantiate this finding, we measured membrane permeability of two nanoparticles in a parallel artificial membrane permeability assay (PAMPA). In this assay, a phospholipid bilayer membrane is used to simulate the lipid bilayer of the cell (Figure 2A).[29] Donor and acceptor wells sandwich the bilayer membrane. After shaking for 3 h, the concentration of nanoparticles in donor, acceptor and the lipid membrane are quantitatively determined by fluorescence measurement. The capability for nanospheres to pass the artificial membrane was about 6-fold higher than that of nanodisks. The membrane retention/permeable ratio for nanodisks was 8-fold higher than that of nanospheres showing the extraordinary membrane association of the nanodisks (Figure 2 B).

Early molecular-dynamics simulation studies using carbon-based nanoparticles as a model predicted that shape and structure significantly affect nanoparticle internalization on a simulated cell membrane. Flat nanoparticles were easier to enter lipid bilayers of the cell membrane while nanospheres tended to impact membrane which eventually led to endocytosis.[30,31] Our experimental data confirmed these simulation results.

Nanodisks, but Not Nanospheres, Predominantly Accumulate in Cell Membranes. The association of nanoparticles to cell membranes may affect the structure of phospholipids that constitute cell membranes.[32] Because nanodisks had much stronger association with cell membranes than nanospheres, we speculated that this might perturb lipid's arrangement in the cell membrane. We used a fluorescent

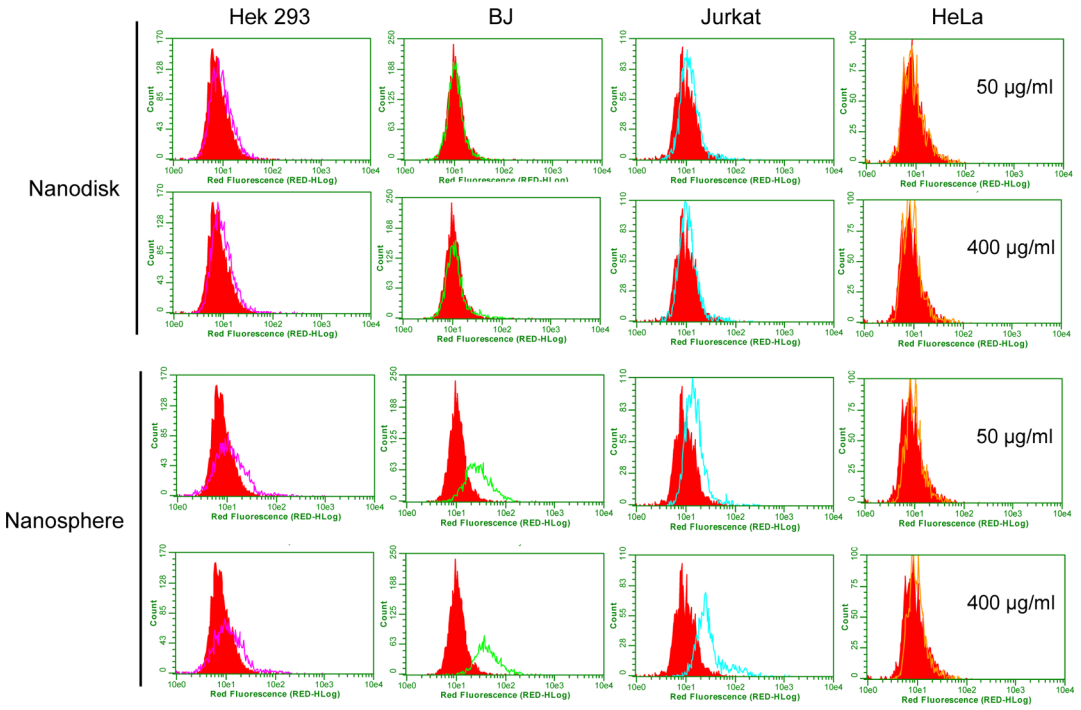

Figure 3. ROS level analysis in four human cell lines after treatment with both polymeric nanoparticles. All cell lines were treated with two nanoparticles at the concentrations of 50 and 400 μg/mL for 24 h and cell culture was incubated with 2 μM DHE for 30 min in dark. ROS was analyzed by flow cytometry.

probe 6-dodecanoyl-2-dimethylaminonaphthalene (Laurdan) to detect the physical state of cell membranes in live cells.[25] Laurdan is a lipophilic polarity-sensitive dye that can be incorporated into the membrane with an even distribution. It aligns in parallel with the hydrophobic lipid chains of the membrane. When the membrane shifts from the gel (ordered) to the fluid (chaotic) phase, its fluorescence intensity is reduced in the short wavelength region (451 nm) while increased in the long wavelength region (490 nm). This caused a decreased generalized polarization (GP) value (see the Materials and methods for details). By analyzing GP values with or without nanoparticles, we found that nanodisks significantly decreased the GP values, whereas nanospheres showed almost no effect compared to untreated cells (Figure 2 C). These results showed that, in contrast to nanospheres, the strong association of nanodisks with the phospholipid bilayer and the significant accumulation of nanodisks in the cell membranes reduced the ordering status of phospholipids. Therefore, fluorescence CLSM study, flow cytometry, PAMPA, and study on lipid ordering convincingly demonstrated that nanodisks bind to cell membranes without significant internalization. Because the thickness of nanodisks (2 nm) is less than the thickness of lipid bilayer (about 5 nm), nanodisks may be buried inside lipid bilayer.

A key property of medicinal nanomaterials is their low cytotoxicity. In order to compare the safety of the nanodisks and nanospheres, induction of reactive oxygen species (ROS) generation, cell apoptosis, and cell cycle perturbation were analyzed in an expanded panel of human cell lines—epithelial cells (Hek293), blood cells (Jurkat), and fibroblasts (BJ).

Unlike Nanospheres, Nanodisks Did Not Induce Cellular ROS. A perturbation on cellular redox balance by nanoparticles is suggested as one of the origins of nanotoxicity.[33] dihydroethidium (DHE) can be oxidized by intracellular superoxide into a fluorescent molecule. We measured nanoparticle-induced intracellular ROS generation by flow cytometry after dihydroethidium (DHE) treatment. We detected small to moderate increases in ROS levels in all four cell lines after exposing to the carboxylated nanopheres under used concentrations (Figure 3). In contrast, no ROS generation was noted after nanodisk treatment. The interactions between nanoparticles and cellular components such as mitochondria[34−36] mediates intracellular ROS generation. The lack of perturbation on intracellular redox balance by nanodisks was expected because they were not evidently internalized by cells.

Nanodisks Did Not Induce Cell Apoptosis or Perturb Cell Cycle. At concentrations below 10 μg/mL, it is reported that negative-charged polystyrene nanoparticles were less toxic than positive-charged ones.[36,37] The cytotoxicity is also dependent on the size of nanoparticles and the cell types.[38] When we used higher concentrations (50 and 400 μg/mL), carboxylated nanospheres induced a significant decrease in cell viability (in HeLa cell, Figure S4 in the Supporting Information) and apoptosis in all four cell lines (Figure 4). In contrast, negligible decrease in cell viability (in HeLa cell, Figure S4 in the Supporting Information) and a very small apoptosis was detected after nanodisk treatment even at a concentration as high as 400 μg/mL (Figure 4). Nanoparticles have been reported to cause cell apoptosis via different cellular signaling pathways,[39,40] ROS induction[40] or binding to cell membrane receptors.[41] Our results, however, excluded the possibility that nanodisks perturbed apoptosis-related cell signaling pathways by binding to cell membrane.

Nanoparticles often perturb cell cycle when internalized by cells. Cell cycle perturbations may be results of DNA damage,[42] abnormal expression of cell cycle−related genes,[43,44] perturbations on cell cycle−related signaling pathways,[45] or interactions with chromosomes.[46] At concentrations below 10 μg/mL, both

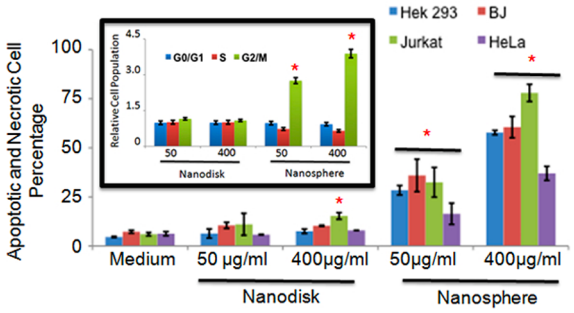

Figure 4. Cell apoptosis and cell cycle analysis after treatment with two polymeric nanoparticles for 24 h. Cells were treated with both nanoparticles at the concentrations of 50 and 400 μg/mL and were stained with Nexin-V reagent and cell cycle reagent for cell apoptosis and cell cycle (cell cycle distribution of BJ cells shown in insert) analysis by flow cytometry.(*p < 0.05, compared to untreated cells).

nanoparticles showed no effects on normal cell cycle progression.[38] At the concentrations of 50 and 400 μg/mL, nanospheres induced cell cycle arrest at G2/M phases in Hek293, BJ and Jurkat cells, and induced G1/S arrest in Jurkat and HeLa cells, while no cell cycle arrest was detected for nanodisks (Figure 4 inset, and Figure S5 in the Supporting Information). This suggested that nanodisks did not affect DNAs, cell cycle-related genes, or related signaling pathways when bound to cell membranes.

CONCLUDING REMARKS

Although an enhanced cell uptake of nanoparticles is sometimes desirable, for example, for drug delivery, the cell membrane binding without uptake is essential for applications like diagnostic imaging and in vivo stem cell tracking. Some surface modifications (for example, coating with PEG[16] or dextran[17]) on nanoparticles can decrease their internalization. However, these nanoparticles cannot be associated or embedded in the cell membranes.[16] Our findings demonstrate that changing nanoparticles to two-dimensional shape provides a practical approach to make cell exterior binders without cell uptake.

Nanomaterials with various shapes have been assembled in recent years.[19,42,47−49] A unique class of nanomaterials is disk-shaped nanomaterials. Nanodisk particles have been made using polystyrene,[19,26] phospholipids,[50] silicon,[51] metallic, or metallic oxide.[52−56] Some of these nanodisks have already shown promising applications in diagnosis.[55] Although the campaign to develop nanodisk materials has progressed rapidly, the understanding of their biological effects has been slow. Here we compared the effects of nanospheres and nanodisks with the same chemical composition, diameter, and surface charges on cell internalization and cell functions. Our investigations using both human cells and artificial membranes show that nanodisks, unlike nanospheres, prefer to localize in phospholipids bilayers and have a very low tendency to penetrate cell membranes. The association of nanodisks to phospholipids and their accumulation in the cell membrane also alter the status of phospholipid ordering. As a result, they have much lower perturbations on cell functions such as cellular ROS generation, cell apoptosis, and cell cycle compared to nanospheres. Cell functions can be controlled or altered by cellular signaling machineries and some receptors are membrane proteins. In the case of polymer nanodisks and nanospheres, the perturbations inside cells show stronger effects on cell functions than membrane perturbations. Because nanodisks can be also made fluorescent or magnetic, the reduced cell internalization makes them promising candidates for applications like in vivo stem cell tracking, stem cell separation, and molecular imaging and tissue engineering.

ASSOCIATED CONTENT

Supporting Information

Size distribution of two nanoparticles, characterizations of nanoparticles after fluorescein labeling, quantification of fluorescence capacity of both nanoparticles, cell membrane association or internalization of both nanoparticles in HeLa cells from a broader view, cell viability in HeLa cells, cell cycle distribution in Hek 293, HeLa, and Jurkat cells 24 h after nanoparticle treatment. This material is available free of charge via the Internet at http://pubs.acs.org.

AUTHOR INFORMATION

Corresponding Author

*Phone: 86-531-88366232. Fax: 86 531-88380029. E-mail: drbingyan@yahoo.com.

Notes

The authors declare no competing financial interest.

ACKNOWLEDGMENTS

We thank Lei Yang, Yannan Ouyan and Gaoxing Su for technique assistance, Jinmei Wu and Qingxin Mu for assistance in graphics. This work was supported by the National Basic Research Program of China (973 Program 2010CB933504), National Natural Science Foundation of China (21077068 and 21137002), NSF (CHE-1012951), NIH (1R21AR060408-01A1), and FedEx Institute of Technology.

REFERENCES

(1) Canton, I.; Battaglia, G. *Chem. Soc. Rev.* **2012**, *41*, 2718−2739.
(2) Sahay, G.; Alakhova, D. Y.; Kabanov, A. V. *J. Controlled Release* **2010**, *145*, 182−195.
(3) Hillaireau, H.; Couvreur, P. *Cell. Mol. Life Sci.* **2009**, *66*, 2873−2896.
(4) Lanzkron, S. M.; Collector, M. I.; Sharkis, S. J. *Blood* **1999**, *93*, 1916−1921.
(5) Voura, E. B.; Jaiswal, J. K.; Mattoussi, H.; Simon, S. M. *Nat. Med.* **2004**, *10*, 993−998.
(6) Ding, D.; Li, K.; Zhu, Z.; Pu, K.-Y.; Hu, Y.; Jiang, X.; Liu, B. *Nanoscale* **2011**, *3*, 1997−2002.
(7) Cromer Berman, S. M.; Walczak, P.; Bulte, J. W. M. *Wiley Interdiscip. Rev.: Nanomed. Nanobiotechnol.* **2011**, *3*, 343−355.
(8) Dahan, M.; Laurence, T.; Pinaud, F.; Chemla, D. S.; Alivisatos, A. P.; Sauer, M.; Weiss, S. *Opt. Lett.* **2001**, *26*, 825−827.
(9) Xie, C.; Yin, D.; Li, J.; Zhang, L.; Liu, B.; Wu, M. *3rd International Nanoelectronics Conference (INEC)*; IEEE: Piscataway, NJ, 2010; pp 1005−1006.
(10) Lee, P.-W.; Hsu, S.-H.; Tsai, J.-S.; Chen, F.-R.; Huang, P.-J.; Ke, C.-J.; Liao, Z.-X.; Hsiao, C.-W.; Lin, H.-J.; Sung, H.-W. *Biomaterials* **2010**, *31*, 2425−2434.
(11) Yukawa, H.; Watanabe, M.; Kaji, N.; Okamoto, Y.; Tokeshi, M.; Miyamoto, Y.; Noguchi, H.; Baba, Y.; Hayashi, S. *Biomaterials* **2012**, *33*, 2177−2186.
(12) Yukawa, H.; Kagami, Y.; Watanabe, M.; Oishi, K.; Miyamoto, Y.; Okamoto, Y.; Tokeshi, M.; Kaji, N.; Noguchi, H.; Ono, K.; Sawada, M.; Baba, Y.; Hamajima, N.; Hayashi, S. *Biomaterials* **2010**, *31*, 4094−4103.
(13) Rand, D.; Ortiz, V.; Liu, Y.; Derdak, Z.; Wands, J. R.; Tatíček, M.; Rose-Petruck, C. *Nano Lett.* **2011**, *11*, 2678−2683.

(14) Peng, X.-H.; Qian, X.; Mao, H.; Wang, A. Y.; Chen, Z. G.; Nie, S.; Shin, D. M. *Int. J. Nanomed.* **2008**, *3*, 311−321.
(15) Ballou, B.; Lagerholm, B. C.; Ernst, L. A.; Bruchez, M. P.; Waggoner, A. S. *Bioconjugate Chem.* **2003**, *15*, 79−86.
(16) Arnida; Malugin, A.; Ghandehari, H. *J. Appl. Toxicol.* **2010**, *30*, 212−217.
(17) Angeles, V.; Magdalena, C.; Alejandro, G. R.; Macarena, C.; Sabino, V.-V.; Carlos, J. S.; María del Puerto, M.; Rodolfo, M. *Nanotechnology* **2009**, *20*, 115103.
(18) Champion, J. A.; Mitragotri, S. *Proc. Natl. Acad. Sci. U.S.A.* **2006**, *103*, 4930−4934.
(19) Tekobo, S.; Pinkhassik, E. *Chem. Commun.* **2009**, *9*, 1112−1114.
(20) Beck, P.; Liebi, M.; Kohlbrecher, J.; Ishikawa, T.; Rüegger, H.; Fischer, P.; Walde, P.; Windhab, E. *Langmuir* **2009**, *26*, 5382−5387.
(21) Canlas, C. G.; Ma, D.; Tang, P.; Xu, Y. *J. Am. Chem. Soc.* **2008**, *130*, 13294−13300.
(22) J.Glover, K.; Whiles, J. A.; Wu, G.; Yu, N.; Deems, R.; Struppe, J. O.; E.Stark, R.; A.Komives, E.; R.Vold, r. *Biophys. J.* **2001**, *81*, 2163−2171.
(23) Sinkó, B.; Kökösi, J.; Avdeef, A.; Takács Novák, K. *Chem. Biodiv.* **2009**, *6*, 1867−1874.
(24) Chen, R.; Huang, G.; Ke, P. C. *Appl. Phys. Lett.* **2010**, *97*, 1−3.
(25) Parasassi, T.; Di Stefano, M.; Ravagnan, G.; Sapora, O.; Gratton, E. *Exp. Cell Res.* **1992**, *202*, 432−439.
(26) Tekobo, S.; Richter, A.; Dergunov, S.; Pingali, S.; Urban, V.; Yan, B.; Pinkhassik, E. *J. Nanopart. Res.* **2011**, *13*, 6427−6437.
(27) Tekobo, S. Dissertation for Doctor of Philosophy Degree. *The University of Memphis*, 2010; p 117.
(28) Cedervall, T.; Lynch, I.; Lindman, S.; Berggård, T.; Thulin, E.; Nilsson, H.; Dawson, K. A.; Linse, S. *Proc. Natl. Acad. Sci. U.S.A.* **2007**, *104*, 2050−2055.
(29) Kansy, M.; Senner, F.; Gubernator, K. *J. Med. Chem.* **1998**, *41*, 1007−1010.
(30) Fiedler, S. L.; Violi, A. *Biophys. J.* **2010**, *99*, 144−152.
(31) Chang, R.; Violi, A. *J. Phys. Chem. B* **2006**, *110*, 5073−5083.
(32) Wang, B.; Zhang, L.; Bae, S. C.; Granick, S. *Proc. Natl. Acad. Sci. U.S.A.* **2008**, *105*, 18171−18175.
(33) Nel, A.; Xia, T.; Mädler, L.; Li, N. *Science* **2006**, *311*, 622−627.
(34) Li, N.; Sioutas, C.; Cho, A.; Schmitz, D.; Misra, C.; Sempf, J.; Wang, M.; Oberley, T.; Froines, J.; Nel, A. *Environ. Health. Perspect.* **2002**, *111*, 455−460.
(35) Karataş, Ö. F.; Sezgin, E.; Aydın, Ö.; Çulha, M. *Colloids Surf., B* **2009**, *71*, 315−318.
(36) Bhattacharjee, S.; de Haan, L.; Evers, N.; Jiang, X.; Marcelis, A.; Zuilhof, H.; Rietjens, I.; Alink, G. *Part. Fibre Toxicol.* **2010**, *7*, 1−12.
(37) Lunov, O.; Syrovets, T.; Loos, C.; Nienhaus, G. U.; Mailänder, V.; Landfester, K.; Rouis, M.; Simmet, T. *ACS Nano* **2011**, Article ASAP.
(38) Liu, Y.; Li, W.; Lao, F.; Liu, Y.; Wang, L.; Bai, R.; Zhao, Y.; Chen, C. *Biomaterials* **2011**, *32*, 8291−8303.
(39) Ristorcelli, E.; Beraud, E.; Mathieu, S.; Lombardo, D.; Verine, A. *Int. J. Cancer* **2009**, *125*, 1016−1026.
(40) Liu, S.; Xu, L.; Zhang, T.; Ren, G.; Yang, Z. *Toxicology* **2010**, *267*, 172−177.
(41) Hirano, S.; Kanno, S.; Furuyama, A. *Toxicol. Appl. Pharmacol.* **2008**, *232*, 244−251.
(42) Zhu, L.; Chang, D. W.; Dai, L.; Hong, Y. *Nano Lett.* **2007**, *7*, 3592−3597.
(43) Ding, L.; Stilwell, J.; Zhang, T.; Elboudwarej, O.; Jiang, H.; Selegue, J. P.; Cooke, P. A.; Gray, J. W.; Chen, F. F. *Nano Lett.* **2005**, *5*, 2448−2464.
(44) Kawata, K.; Osawa, M.; Okabe, S. *Environ. Sci. Technol.* **2009**, *43*, 6046−6051.
(45) Mu, Q.; Du, G.; Chen, T.; Zhang, B.; Yan, B. *ACS Nano* **2009**, *3*, 1139−1144.
(46) Kang, B.; Mackey, M. A.; El-Sayed, M. A. *J. Am. Chem. Soc.* **2010**, *132*, 1517−1519.
(47) Sun, Y.; Xia, Y. *Science* **2002**, *298*, 2176−2179.
(48) Geng, Y.; Discher, D. E. *J. Am. Chem. Soc.* **2005**, *127*, 12780−12781.
(49) Kohler, J. M.; Romanus, H.; Hubner, U.; Wagner, J. *J. Nanomater.* **2007**, *2007*, 2−2.
(50) Ritchie, T.; Grinkova, Y.; Bayburt, T.; Denisov, I.; Zolnerciks, J.; Atkins, W.; Sligar, S. *Methods Enzymol.* **2009**, *464*, 211−231.
(51) Kubota, T.; Hashimoto, T.; Ishikawa, Y.; Samukawa, S.; Miura, A.; Uraoka, Y.; Fuyuki, T.; Takeguchi, M.; Nishioka, K.; Yamashita, I. *Appl. Phys. Lett.* **2006**, *89*, 233127.
(52) Cowburn, R. P.; Koltsov, D. K.; Adeyeye, A. O.; Welland, M. E.; Tricker, D. M. *Phys. Rev. Lett.* **1999**, *83*, 1042−1045.
(53) Hengstmann, T. M.; Grundler, D.; Heyn, C.; Heitmann, D. *J. Appl. Phys.* **2001**, *90*, 6542−6544.
(54) Xu, C. X.; Sun, X. W.; Dong, Z. L.; Yu, M. B. *Appl. Phys. Lett.* **2004**, *85*, 3878−3880.
(55) Qin, L.; Banholzer, M. J.; Millstone, J. E.; Mirkin, C. A. *Nano Lett.* **2007**, *7*, 3849−3853.
(56) Fang, Z.; Cai, J.; Yan, Z.; Nordlander, P.; Halas, N. J.; Zhu, X. *Nano Lett.* **2011**, *11*, 4475−4479.